Effect of process parameters on separation efficiency in a deterministic lateral displacement device

Behrouz Aghajanloo [a,b,c], David W. Inglis [d], Fatemeh Ejeian [b], Alireza Fadaei Tehrani [a,*], Mohammad Hossein Nasr Esfahani [b,*], Mohsen Saghafian [a], Giancarlo Canavese [c], Simone L. Marasso [c,e]

[a] Department of Mechanical Engineering, Isfahan University of Technology, Isfahan, Iran
[b] Department of Animal Biotechnology, Cell Science Research Center, Royan Institute for Biotechnology, ACECR, Isfahan, Iran
[c] DISAT, Politecnico di Torino, Turin, Italy
[d] School of Engineering, Macquarie University, Sydney, Australia
[e] CNR-IMEM, Parma, Italy

ARTICLE INFO

ABSTRACT

Deterministic lateral displacement (DLD) is a hydrodynamic method known for its high-resolution sorting of particles. It achieves this through a periodic array of obstacles and laminar flow that passively directs particles along in two different directions depending on the particles' diameter. Many prior publications have been dedicated to the structural and geometrical development of DLD arrays to improve separation performance; however, a successful separation requires much more than a well-designed array. This paper shows how separation performance is affected by process parameters. For this purpose, the design and fabrication of a DLD device are described. Then three experiments show how process parameters affect the performance of the device. The first experiment uses dye solutions to visualize the formation of a hydrodynamically focused sample stream. The second experiment shows that the particle separation performance (of 7- & 15-μm particles) is affected by the way output fluids are collected. Finally, the third experiment looks at the particle separation efficiency as the input flow rates and the ratio of buffer to sample are changed. The results show that the proper range for buffer and sample flow rate in this device is 1–10 and 0.1–1 (μl/min), respectively. The buffer to sample flow rate ratio of 10 gives the highest separation efficiency, but at a lower sample throughput. The optimized values are specific for our device but demonstrate processes that we believe are universal for DLD separations.

© 2022 Published by Elsevier B.V.

1. Introduction

Deterministic Lateral Displacement (DLD) is a hydrodynamic separation method that uses periodic flow patterns created by an array of obstacles. Ever since the concept of DLD was described by Huang et al. [1], a great deal of analytical, numerical, and practical studies have been conducted for improving and understanding the separation performance. Most of these studies have investigated array design parameters including DLD array geometry and surface properties [2–10], layout [11–16] and boundaries [17–19]. However, other parameters also affect the separation efficiency. They are process parameters [20], about which, there is little explicit investigation.

After chip fabrication, there are very few ways to make changes in separation performance. While Beech and Tegenfeldt [21], stretched DLD devices to change the critical diameter, still post-fabrication modifications are rare. The main adjustable settings for DLD setups are input flow rates. Typically, two inputs are used: buffer and sample. Buffer flow on either side of the sample flow is desirable to create flow focusing and to minimize side-wall effect [22]. The appropriate flow rates for buffer and sample depend on various factors such as array width and depth, widths of buffer and sample inlets, widths of product and waste outlets, and risk of clogging/aggregation, but the best value is frequently determined experimentally. A more fundamental consideration than the absolute values, is the ratio of buffer to sample flow rate. This is because the sample flow stream confinement is determined by their ratio, instead of their absolute values.

The flow pattern in the DLD array is also sensitive to flow perturbation at the outlets. This means that the method of collecting the product and waste fluid may affect device performance.

Table 1
Array parameters.

	Row shift fraction	Period	Array tilt angle	Gap width	Channel depth	Critical diameter	Post Diameter	Pitch
Symbol	ε	N	θ	G (μm)	E (μm)	D_c (μm)	D_p (μm)	λ (μm)
Value	0.05	20	2.86°	30	30	10	30	60

Table 2
Device parameters.

	Left buffer columns	Sample columns	Right buffer columns	Product(large) columns	Waste (small) columns	Whole columns	Arraywidth (μm)	Array length (μm)	Redundancy
Value	47%	27%	26%	27%	73%	67	4030	21,000	21%

Manual micro-pipetting from on-chip outlet reservoirs and fixed tubing from the chip to collection tubes are the two most common techniques that are using to collect the output fluids [23–26].

This work aims to explore how process parameters influence the flow stream pattern which affects DLD performance. Thereby, a qualitative visualization of flow focusing, and a quantitative analysis of particle separation as flow rates and ratios are changed, have been conducted.

2. Materials and methods

2.1. Array design

The device was designed to separate large non-adherent mammalian cells (like circulating tumor cells with average diameter of around 12-μm) from normal white blood cells (like Lymphocytes with a typical diameter of around 8-μm). An empirical equation relating gap size and critical diameter established by Davis [27] for circular obstacles has been used to create a rhombic array [28] with a critical diameter of 10-μm and a row shift fraction of 0.05. This gives a gap of 30-μm (three times the critical diameter) [5,12,29]. Also, the boundary modification formula established by Inglis has been considered to design the array as productive as

possible [18,30]. An aspect ratio of 1 for pillars is suitable because it will provide reliable fabrication across the entire array and an acceptable fluidic throughput. The array's geometrical parameters are shown in Table 1.

2.2. Device parameters

The remaining parameters of the array, including the whole width and length of array and their budgeting regarding inlets and outlets, are reported in Table 2. If large particles always follow the array angle, particles entering the array from the left edge of the sample inlet, will be upstream of the large particle outlet after 18 mm of array. The array is made 34% longer than this for redundancy and safety margin. Finally, the proposed layout has been prepared by CAD software which is shown in Fig. 1.

2.3. Process parameters

Buffer inlets were used on either side of the sample. It is a well-known technique which hydrodynamically focuses the sample stream and keeps the sample away from the lateral boundaries where separation is non-ideal. To predict the flow rate, prerequisite values such as fluid resistance and pressure [27] have been
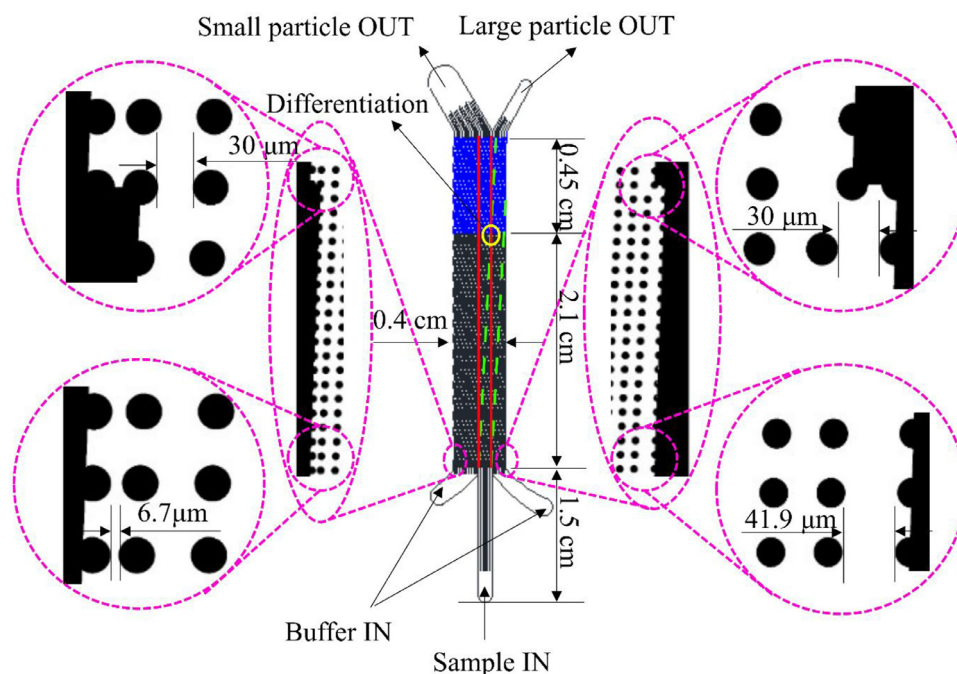

Fig. 1. 2D design of DLD device. Blue part: Engineering safety margin, Green dashed line: Bump mode trajectory, Red solid line: Zigzag mode trajectory.
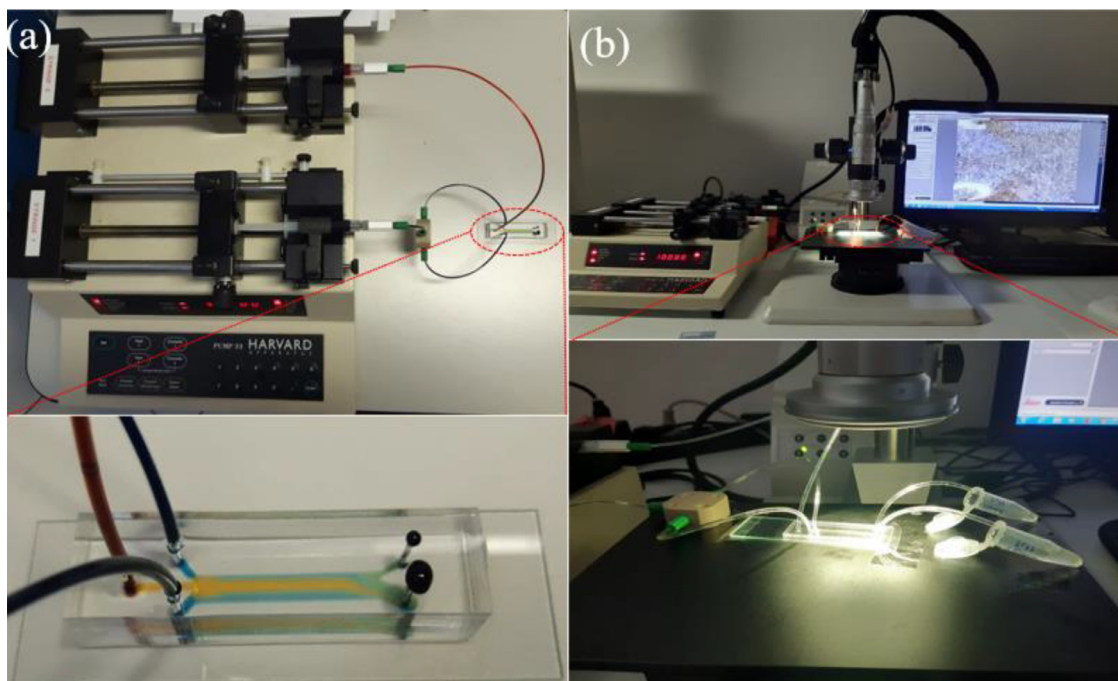
Fig. 2. DLD experiment setup comprised of syringe pump and DLD microchip for a) Qualitative investigation with food dye solution, b) Quantitative investigation with microbeads, collecting outputs by silicon carrier tubes.

Table 3
Process parameters.

	Viscosity	Volumetric flow rate	Sample volume	Pressure	Array fluidic resistance	Cycle time
Symbol	μ (Pa. s)	Q (μL/min)	V (μL)	P (kPa)	R (Pa. s/m^3)	T (min)
Value	0.001	10	1000	50	2.4e12	100

obtained by fluid dynamics analytical calculations which are given in Table 3.

2.4. Device fabrication

A Chromium mask has been printed by Laser writer (Microtech, Italy). Afterwards, a standard recipe for SU8 UV photolithography has been applied using a mask aligner system (Neutronix quintel, USA) to fabricate the master mold with a thickness of 30 μm. Then, PDMS replica molding has been performed employing the master mold [31], which was treated by a salinization step [32]. This was followed by making the outlet holes via 1.5-mm biopsy punch and bonding to a standard microscope slide using oxygen plasma treatment (Diener electronics, Germany) [33].
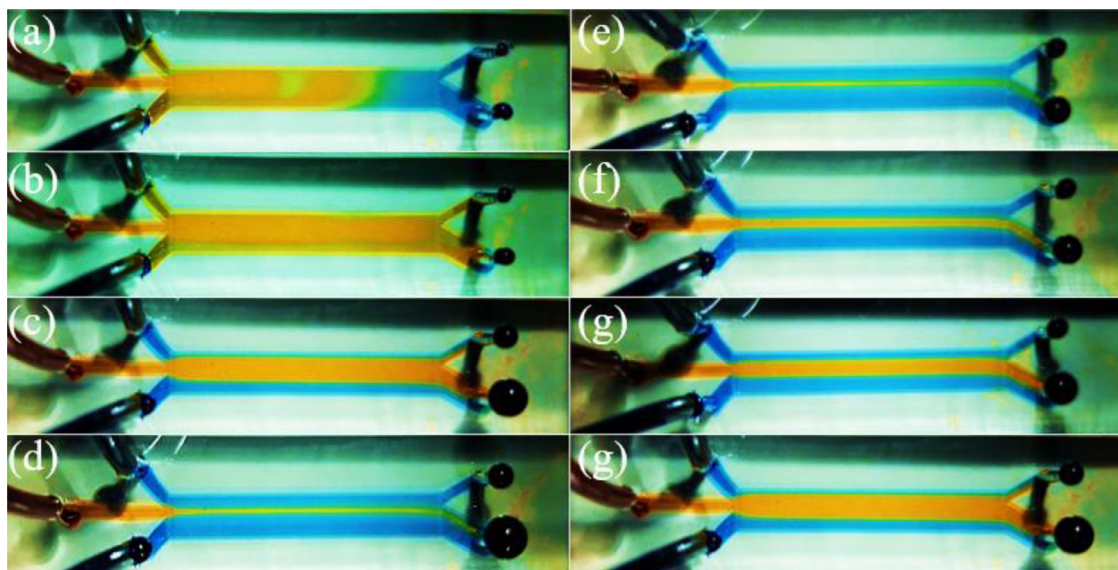

Fig. 3. a) Time-lapse imaging of flow focusing. Left: Flow focusing at 5:0.5 μl/min buffer/sample flow rate ratio after a) 0 b) 30 c) 60 d) 120 s. Right: Focused flow regime after 2 min in e) 5:0.5 f) 5:1 g) 5:2.5 h) 5:5 μl/min buffer/sample flow rate ratio.

2.5. Device preparation

Bubble generation is a challenge in microfluidic devices. It is especially critical in DLD arrays where, once in the array, they are very difficult to remove. The possibility and consequences of particles sticking to the features is similarly problematic in DLD devices. Thus, we had to apply surface pretreatment before running the device. This step has been done by wetting and soaking the device in 0.1% (v/v) Tween 20 in de-ionized water solution under vacuum for 30 min [34].

2.6. Qualitative experiments

To demonstrate the relation between process factors and flow distribution, first experiments using food dye (Fugar, Italy) have been carried out. Buffer and sample syringes have been filled with colored aqueous solutions of blue and yellow dye (respectively) and placed in two equal length channels of a syringe pump (Harvard, USA) (Fig. 2-a). The buffer tube splits into two tubes using a T-junction before connecting to the chip. The feeding tubes' tips were pushed into the inlet holes of pre-wetted device gently, with the liquid meniscus at the tip to prevent the introduction of bubbles.

2.7. Sample preparation

Seven- and 15-µm fluorescent microbeads with specification range of 6.5–7.5 µm and 14.5–15.5 µm respectively (Bang laboratories, USA) with the batch concentration of 15×10^6 (particles/ml) were diluted first by 1:100 ratio in 0.1% (v/v) aqueous Tween 20 solution. Then mixed in a 4:1 ratio of 7- and 15-µm beads respectively, followed by final 10x dilution in 0.1% Tween 20 solution. This gives final concentration of 12,000 particles/ml of 7-µm beads and 3000 particles/ml of 15-µm beads.

2.8. Quantitative experiments

Quantitative experiments with fluorescent microbeads have also been conducted. The chip was prepared in the same way as described in Section 2.5, but the syringes were filled then with undyed 0.1% Tween 20 solution. The sample syringe contained a mixture of beads that had recently been thoroughly vortexed. Next, the degassed microchip filled with surfactant solution has been connected to tubing likewise described in Section 2.6, and fixed on the microscope stage (Leica stereomicroscope, Italy).

2.9. Output collection

Two different product collection methods have been tested. First, fluid exiting the chip was periodically pipetted from outlet reservoirs (1 mm in diameter and 9 mm in height) into collection tubes, a method hereafter called "Micro-pipetting". Secondly, short silicon tubes connected the outlets to separate Eppendorf tubes, a method hereafter called "Carrier tube" (Fig. 2-b).

3. Experimental results and discussion

3.1. Qualitative results

Following the qualitative experimental details described earlier (Section 2.6), images of how flow rate affects the macroscopic flow patterns in the device have been presented. A flow establishment period between initiation of flow at the syringe pump and steady-state conditions was observed. An illustration of this phase is depicted in Fig. 3 (Left). It clearly shows that buffer focuses the sample to create a sharp interface between two miscible fluid streams after a transition period.
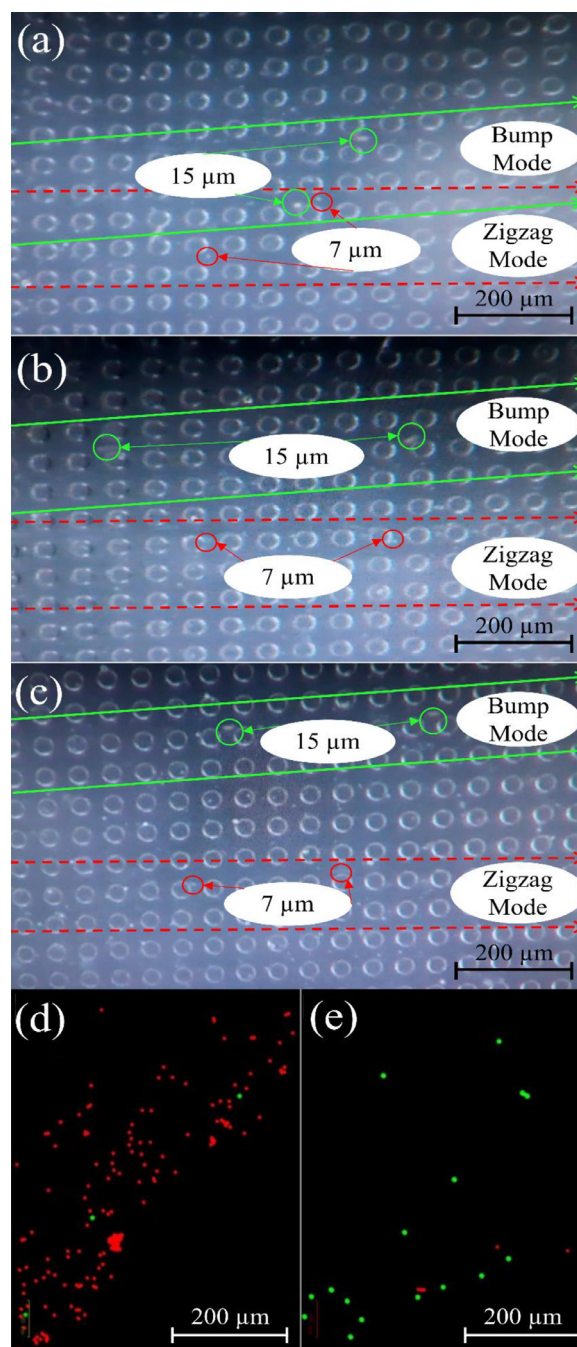

Fig. 4. Microbeads in the DLD array. a) Before, b) near, c) after differentiation point (onset of safety margin region). Green solid line: Bump mode trajectory, Red dashed line: Zigzag mode trajectory.
Fluorescent images of collected outputs from d) small outlet, e) large outlet. Images are from an experiment done in a 5:2.5 µl/min buffer/sample flow rate ratio. 7-µm particles are red, and 15 µm particles are green.

This experiment has been carried out at 4 different flow rate ratios, keeping the buffer flow rate fixed at 5 µl/min. Fig. 3 (Right) shows the flow patterns for these 4 ratios after 120 s (steady state).

According to Fig. 3 (Right), it is clearly visible that the ratio of 2 between buffer to sample flow rate (5:2.5 µl/min) is the threshold for ensuring that small particles go to the waste outlet. If the ratio is increased, for example to a ratio of 5:5, the sample enters both outlets, contaminating the product. If the sample flow rate is decreased, for example to a ratio of 5:1, the product is not contaminated, but the device is not processing sample at its maxi-
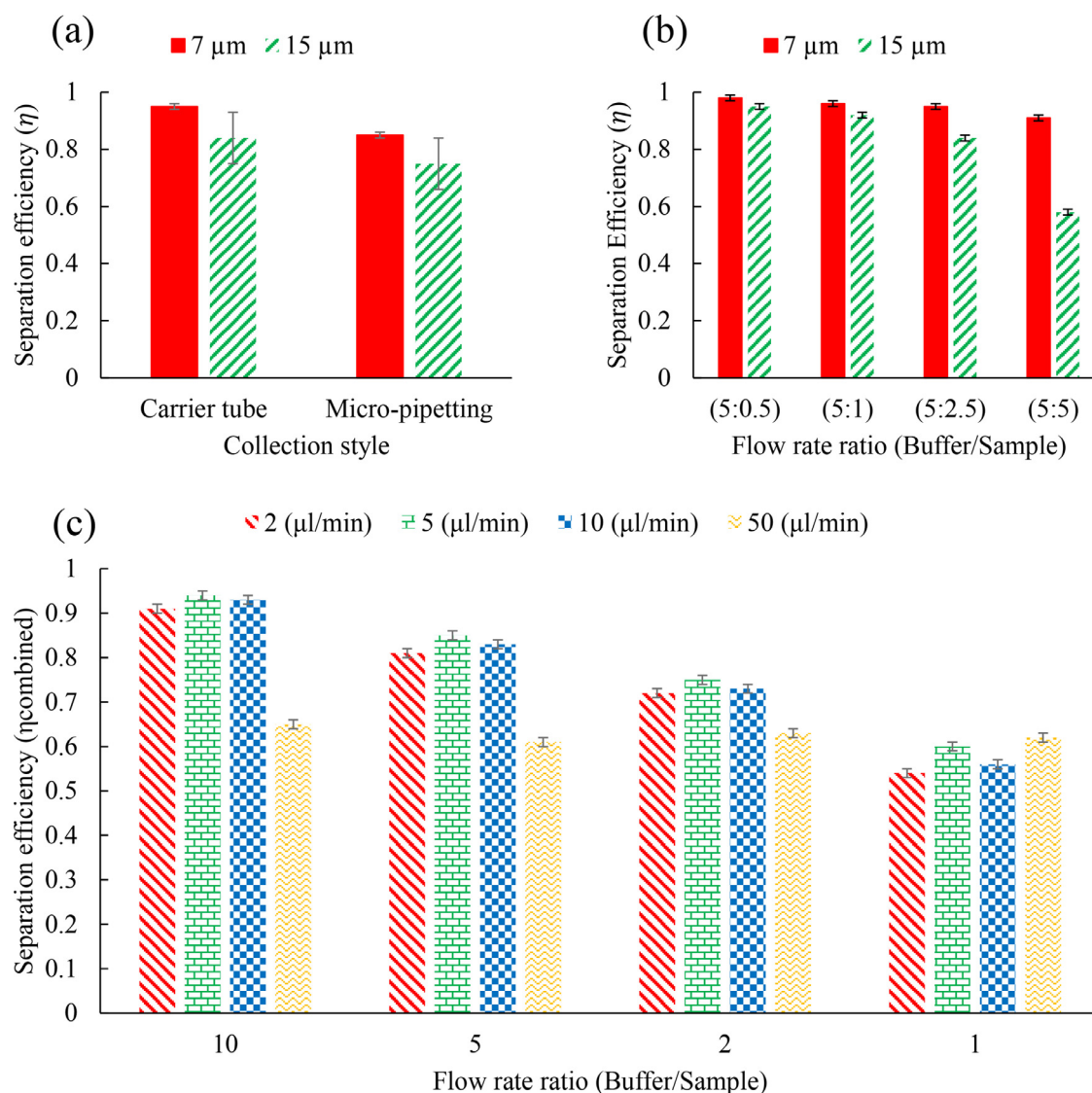
Fig. 5. a) Separation efficiency vs collection style with a 5:2.5 µl/min buffer/sample flow rate ratio, b) Separation efficiency vs buffer/sample flow rate ratio. Graphs are correlated to "carrier-tube" output collecting style, c) Combined separation efficiency of 15- and 7-µm beads versus buffer/sample flow rate ratio (error bars are +/- 1 standard deviation of repeated experiments). Legend demonstrates buffer flow rates.

mum rate. In a real-world situation there is a compromise between the sample fluid throughput and the output purity. In other words, higher buffer/sample flow rate ratio is expected to result in higher purity but lower throughput. Thus, the proper ratio depends on desired requirements.

3.2. Quantitative results

In the following, the action of distinct-sized particles is reported. The threshold flow rate ratio of 5:2.5 µl/min has been selected for this work. Fig. 4-a to 4-c shows larger particles move up the array in bump mode, while the smaller particles traverse the array largely undeflected (Movie S1). Fluorescent images of microbeads collected at both outlets were taken under inverted fluorescence microscope (Nikon, USA) and post-processed by ImageJ for counting (Fig. 4-d and 4-e).

We have sought to measure the effect of two major process parameters on separation efficiency. The first is the method of collecting fluid from the chip (as described earlier), and the second is the flow rates of the sample and buffer. Separation efficiency (η) is here defined as the number of desired particles in its dedicated

outlet per the total number of that particle in both outlets. For example, the separation efficiency for 7-µm particles is:

$$\eta_7 = \frac{N_{7\,small\,outlet}}{N_{7\,small\,outlet} + N_{7\,large\,outlet}}$$

Fig. 5-a shows the separation efficiency as a function of the fluid collection style. Both the efficiency and repeatability of separation are better when the output is collected using fixed tubes Micro-pipetting increases the risk of perturbation due to abrupt fluid suction, and causes an imbalance in the height of fluid and meniscus curvature in the outlet reservoirs. This causes changes to the flow patterns near the end of the array and may lead particles to enter the wrong outlet. Using larger diameter outlet reservoirs would reduce changes in head pressure and pressure from meniscus curvature, but large reservoirs are harder to make, collect dust from the environment, and have higher evaporation rates. Carrier-tube collecting style is used for the following experiments.

Separation efficiency of 7- and 15-µm beads in various buffer/sample flow rate ratios [in fixed buffer flow rate on 5 (µl/min)] have been investigated. The separation efficiency of each
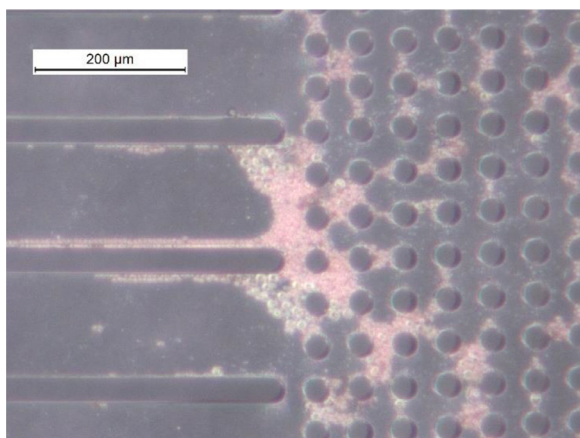
Fig. 6. Microbead accumulation at the beginning of the array at a flow rate ratio of 10 and a buffer flow rate of 50 μl/min.

particle diameter as a function of the flow rate ratio is presented in Fig. 5-b.

At a flow rate ratio of 5:5 the separation efficiency of the 15-μm particles (η_{15}) is significantly reduced. At this ratio, the sample stream is too wide, and a significant number of 15-μm particles enter the DLD array too far to one side. The array is not long enough to displace them into the correct outlet. Increasing the array length (more redundancy) could restore the high efficiency at this ratio. As the ratio continues to decrease, the separation efficiency of the 15-μm (η_{15}) particles is expected to drop. Further at a flow rate ratio of 0:1 (no buffer flow), we expect η_{15} to reach 0.3.

The most important measurement in DLD device is the separation of the large particles from the small particles. The location of just the 15-μm particles, or just the 7-μm particles by themselves is not adequate information to confirm that one thing has been separated from the other. A better measure of the overall separation performance is the product of the two separation efficiencies. This combined efficiency ($\eta_{\text{combined}} = (\eta_7)(\eta_{15})$) as a function of flow ratio and rate is shown in Fig. 5-c.

There is a steady decrease in efficiency with decreasing flow rate ratio. At the flow rate ratio of 10 there is a significant drop in performance at the highest buffer flow rate of 50 μl/min. This drop is likely due to an accumulation of particle blockages which are observed in beginning of the array (Fig. 6). Near stationary bead accumulations, the fluid must deviate from the vertical flow direction that is necessary for bumping. Large blockages reduce the effective length of the array and prevent large beads from bumping to the large outlet. We observe this effect at a flow rate that 5 times higher than the next largest rate of 10 μl/min. Because all experiments are run for 10 min, this experiment processes five times more beads. Much less clogging is observed after 10 min at the lower flow rates (not shown).

4. Conclusion

We have shown how the performance of a DLD array is influenced by operational factors including flow values/ratios as well as output collection style (micro-pipetting vs carrier-tube). Two types of experiments have been conducted: qualitative (using dye solutions to visually demonstrate fluid behavior) and quantitative (using fluorescent microbeads) experiments. Qualitative experiments demonstrate a transition phase between commencement of flow and establishment of the steady state hydrodynamic focusing that is needed for good separation. Quantitative experiments with fluorescent microbeads showed that (i) sample collection using fixed tubing was much more reliable than manual pipetting, and (ii)

flow rate ratio has a stronger effect on separation efficiency than the absolute values of flow rates. These conclusions are likely true for most DLD devices, though the exact sensitivity will depend on device and experimental parameters. This work demonstrates appropriate considerations and assumptions needed for designing the device as well as useful operational parameters for running the separation.

Declaration of Competing Interest

The authors declare that they have no known competing financial interests or personal relationships that could have appeared to influence the work reported in this paper.

CRediT authorship contribution statement

Behrouz Aghajanloo: Conceptualization, Methodology, Validation, Formal analysis, Investigation, Writing – original draft, Writing – review & editing, Visualization. **David W. Inglis:** Conceptualization, Methodology, Validation, Resources, Writing – review & editing, Supervision, Project administration. **Fatemeh Ejeian:** Methodology, Validation, Writing – review & editing, Supervision, Project administration. **Alireza Fadaei Tehrani:** Writing – review & editing, Supervision, Project administration, Funding acquisition. **Mohammad Hossein Nasr Esfahani:** Writing – review & editing, Supervision, Project administration, Funding acquisition. **Mohsen Saghafian:** Supervision. **Giancarlo Canavese:** Writing – review & editing, Supervision, Project administration, Funding acquisition. **Simone L. Marasso:** Writing – review & editing, Supervision, Project administration, Funding acquisition.

Acknowledgments

Supplementary materials

Supplementary material associated with this article can be found, in the online version, at doi:10.1016/j.chroma.2022.463295.

References

[1] L.R. Huang, E.C. Cox, R.H. Austin, J.C. Sturm, Continuous particle separation through deterministic lateral displacement, Science 304 (5673) (2004) 987–990 (80-).

[2] M. De Pra, W.T. Kok, P.J. Schoenmakers, Topographic structures and chromatographic supports in microfluidic separation devices, J. Chromatogr. A 1184 (1–2) (2008) 560–572 Mar 14.

[3] E. Pariset, J. Berthier, C. Pudda, D. Gosselin, F. Navarro, B. Icard, et al., Deterministic Lateral Displacement (DLD): finite element modeling and experimental validation for particle trajectory and separation, TechConnect Briefs 3 (2017) 142–145.

[4] S. Feng, A.M. Skelley, A.G. Anwer, G. Liu, D.W. Inglis, Maximizing particle concentration in deterministic lateral displacement arrays, Biomicrofluidics 11 (2) (2017) 024121.

[5] D.W. Inglis, J.A. Davis, R.H. Austin, J.C. Sturm, Critical particle size for fractionation by deterministic lateral displacement, Lab Chip 6 (5) (2006) 655–658.

[6] M. Heller, H. Bruus, F. Okkels, N. Mortensen, Design Optimization of Bumper Arrays Using Topology Optimization, Technical University of Denmark, 2006.

[7] A. Khater, M. Sabry, H. AbdelMeguid, Design Parameters for deterministic lateral displacement separation technique in biomems, in: Proceedings of the 4th European Conference on Microfluidics, Limerick, Republic of Ireland, 2014.

[8] J.C. Hyun, J. Hyun, S. Wang, S. Yang, Improved pillar shape for deterministic lateral displacement separation method to maintain separation efficiency over a long period of time, Sep. Purif. Technol. 172 (2017) 258–267.

[9] S. Ranjan, K.K. Zeming, R. Jureen, D. Fisher, Y. Zhang, DLD pillar shape design for efficient separation of spherical and non-spherical bioparticles, Lab Chip 14 (21) (2014) 4250–4262.

[10] J. Wei, H. Song, Z. Shen, Y. He, X. Xu, Y. Zhang, et al., Numerical study of pillar shapes in deterministic lateral displacement microfluidic arrays for spherical particle separation, IEEE Trans. Nanobiosci. 14 (6) (2015) 660–667.

[11] B. Rezaei, M. Moghimi Zand, R. Javidi, Numerical simulation of critical particle size in asymmetrical deterministic lateral displacement, J. Chromatogr. A 1649 (2021) 462216 Jul 19.

[12] J.A. Davis, D.W. Inglis, K.J. Morton, D.A. Lawrence, L.R. Huang, S.Y. Chou, et al., Deterministic hydrodynamics: taking blood apart, Proc. Natl. Acad. Sci. USA 103 (40) (2006) 14779–14784.

[13] Q. Wei, Y.Q. Xu, X.Y. Tang, F.B. Tian, An IB-LBM study of continuous cell sorting in deterministic lateral displacement arrays, Acta Mech. Sin. 32 (6) (2016) 1023–1030.

[14] R. Vernekar, T. Krüger, K. Loutherback, K.W. Morton, D. Inglis, D.W Inglis, Anisotropic permeability in deterministic lateral displacement arrays, Lab Chip 17 (19) (2017) 3318–3330.

[15] S.R. Risbud, G. Drazer, Directional locking in deterministic lateral-displacement microfluidic separation systems, Phys. Rev. E Stat. Nonlinear Soft Matter Phys. 90 (1) (2014) 012302.

[16] H. Mohamed, J.N. Turner, M. Caggana, Biochip for separating fetal cells from maternal circulation, J. Chromatogr. A 1162 (2) (2007) 187–192 Aug 31.

[17] S. Feng, A. M.Skelley, D Inglis, Solving the DLD boundary problem using iterative CFD — Macquarie University, in: Proceedings of the International Conference on Miniaturized Systems for Chemistry and Life Sciences (MicroTAS 2018), Chemical and Biological Microsystems Society, Kaohsiung, Taiwan, 2018, pp. 2063–2066.

[18] D.W. Inglis, Efficient microfluidic particle separation arrays, Appl. Phys. Lett. 94 (1) (2009) 013510.

[19] A. Ebadi, M.J. Farshchi Heydari, R. Toutouni, B. Chaichypour, M. Fathipour, K Jafari, Efficient paradigm to enhance particle separation in deterministic lateral displacement arrays, SN Appl. Sci. 1 (10) (2019) 1–9 2019 110Sep 9.

[20] E. Henry, Cell Sorting in Deterministic Lateral Displacement Devices, University of Cologne, 2017.

[21] J.P. Beech, J.O. Tegenfeldt, Tuneable separation in elastomeric microfluidics devices, Lab Chip 8 (5) (2008) 657–659.

[22] T. Salafi, Y. Zhang, Y. Zhang, A review on deterministic lateral displacement for particle separation and detection, Nano-Micro Lett. 11 (2019) 3 Vol.SpringerOpen.

[23] F. Barbaresco, M. Cocuzza, C.F. Pirri, S.L. Marasso, Application of a micro free-flow electrophoresis 3D printed Lab-on-a-Chip for micro-nanoparticles analysis, Nanomaterials 10 (2020) 1277 2020 Jun 30;10(7):1277.

[24] Z. Liu, F. Huang, J. Du, W. Shu, H. Feng, X. Xu, et al., Rapid isolation of cancer cells using microfluidic deterministic lateral displacement structure, Biomicrofluidics 7 (1) (2013) 011801 Feb 4.

[25] J. Beech, Microfluidics Separation and Analysis of Biological Particles, Lund University, 2011.

[26] R. Huang, T.A. Barber, M.A. Schmidt, R.G. Tompkins, M. Toner, D.W. Bianchi, et al., A microfluidics approach for the isolation of nucleated red blood cells (NRBCs) from the peripheral blood of pregnant women, Prenat. Diagn. 28 (10) (2008) 892–899 Oct.

[27] J.A. Davis, Microfluidic Separation of Blood Components Through Deterministic Lateral Displacement, Princeton University, 2008.

[28] J. McGrath, M. Jimenez, H. Bridle, Deterministic lateral displacement for particle separation: a review, Lab Chip 14 (21) (2014) 4139–4158.

[29] D.W. Inglis, M. Lord, R.E. Nordon, Scaling deterministic lateral displacement arrays for high throughput and dilution-free enrichment of leukocytes, J. Micromech. Microeng. 21 (5) (2011) 054024.

[30] D. Inglis, R. Vernekar, T. Krüger, S. Feng, The fluidic resistance of an array of obstacles and a method for improving boundaries in deterministic lateral displacement arrays, Microfluid. Nanofluid. 24 (3) (2020) 1–8 Mar 1.

[31] J. Friend, L. Yeo, Fabrication of microfluidic devices using polydimethylsiloxane, Biomicrofluidics 4 (2) (2010).

[32] M. Joshi, R. Pinto, V.R. Rao, S. Mukherji, Silanization and antibody immobilization on SU-8, Appl. Surf. Sci. 253 (6) (2007) 3127–3132 Jan 15.

[33] Borók A., Laboda K., Biosensors A.B., 2021 U. PDMS bonding technologies for microfluidic applications: a review. mdpi.com. 2021.

[34] R.S. Pawell, D.W. Inglis, T.J. Barber, R.A. Taylor, Manufacturing and wetting low–cost microfluidic cell separation devices, Biomicrofluidics 7 (5) (2013) 056501 Sep 11.